Swiss J Geosci (2017) 110:793–809
DOI 10.1007/s00015-017-0278-z

Chronology of Quaternary terrace deposits at the locality Hohle Gasse (Pratteln, NW Switzerland)

Anne Claude[1] · Naki Akçar[1] · Susan Ivy-Ochs[2] · Fritz Schlunegger[1] · Philippe Rentzel[3] · Christine Pümpin[3] · Dmitry Tikhomirov[1,5] · Peter W. Kubik[2] · Christof Vockenhuber[2] · Andreas Dehnert[4] · Meinert Rahn[4] · Christian Schlüchter[1]

Received: 19 June 2016 / Accepted: 14 June 2017 / Published online: 14 July 2017

Abstract The Quaternary stratigraphy of the Alpine Foreland consists of distinct terrace levels, which have been assigned to four morphostratigraphic units: Höhere (Higher) Deckenschotter, Tiefere (Lower) Deckenschotter, Hochterrasse (High Terrace) and Niederterrasse (Lower Terrace). Here, we focus on the terrace gravels at Hohle Gasse, SSE of Pratteln near Basel, which are mapped as Tiefere Deckenschotter. Petrographic and morphometric data established from clasts allowed to infer the transport mechanisms and sources of the gravels. Sedimentological analyses indicate that the gravels were transported by a braided river and deposited in a distal glaciofluvial setting. In addition, it can be shown that the majority of the clasts display multiple reworking and only a minority maintained a distinct glaciofluvial shape. Cosmogenic multi-isotope dating using ^{10}Be and ^{36}Cl allowed direct dating of the sediments at the study site. A depth-profile age of 270^{+830}_{-190} ka for ^{10}Be was achieved for the deposits at Hohle Gasse. Unfortunately, no age could be modelled from the ^{36}Cl concentrations as the blank correction was too high. Furthermore, this age proves that the studied terrace level should be assigned to the morphostratigraphic unit Hochterrasse.

Keywords Cosmogenic · ^{10}Be · Depth-profile dating · Hochterrasse · Deckenschotter

Editorial handling: A. G. Milnes.

✉ Anne Claude
anne.claude@geo.unibe.ch

[1] Institute of Geological Sciences, University of Bern, Bern, Switzerland

[2] Laboratory of Ion Beam Physics, ETH Zurich, Zurich, Switzerland

[3] Integrative Prehistory and Archaeological Science (IPNA), Basel University, Basel, Switzerland

[4] Swiss Federal Nuclear Safety Inspectorate ENSI, Brugg, Switzerland

[5] Present Address: Department of Physics and Astronomy, Aarhus University, Århus, Denmark

1 Introduction

The whole chronology of glaciations of the Alps is based on morphostratigraphy with terraces (Penck and Brückner 1909). The chronology of terrace sequences in the northern Alpine Foreland is however not completely established (Fig. 1). Therefore, numerical dating of the terraces is fundamental for reconstructing the sequence of glaciations of the Alps. The terraces have been categorized into the units Höhere Deckenschotter (HDS; Higher Deckenschotter), Tiefere Deckenschotter (TDS; Lower Deckenschotter), Hochterrasse (HT; High Terrace) and Niederterrasse (NT; Lower Terrace) based on their altitude above the recent valley floor as well as on distinct sedimentological characteristics (Du Pasquier 1891; Gutzwiller 1894; Penck and Brückner 1909; Frei 1912; Hantke 1978; Haldimann et al. 1984; Graf 1993). The Deckenschotter units HDS and TDS lie uncomformably on Tertiary Molasse or Mesozoic carbonate bedrock. A significant phase of incision separated both units resulting in a difference in elevation of their base layer (Graf 1993, 2009). The HDS deposits have currently been dated to the early Pleistocene (Akçar et al. 2014; Claude et al. 2017; Akçar et al. in press). Palaeomagnetic studies in an abandoned TDS quarry in Allschwil (ca. 10 km W of Pratteln; Fig. 2) show reverse

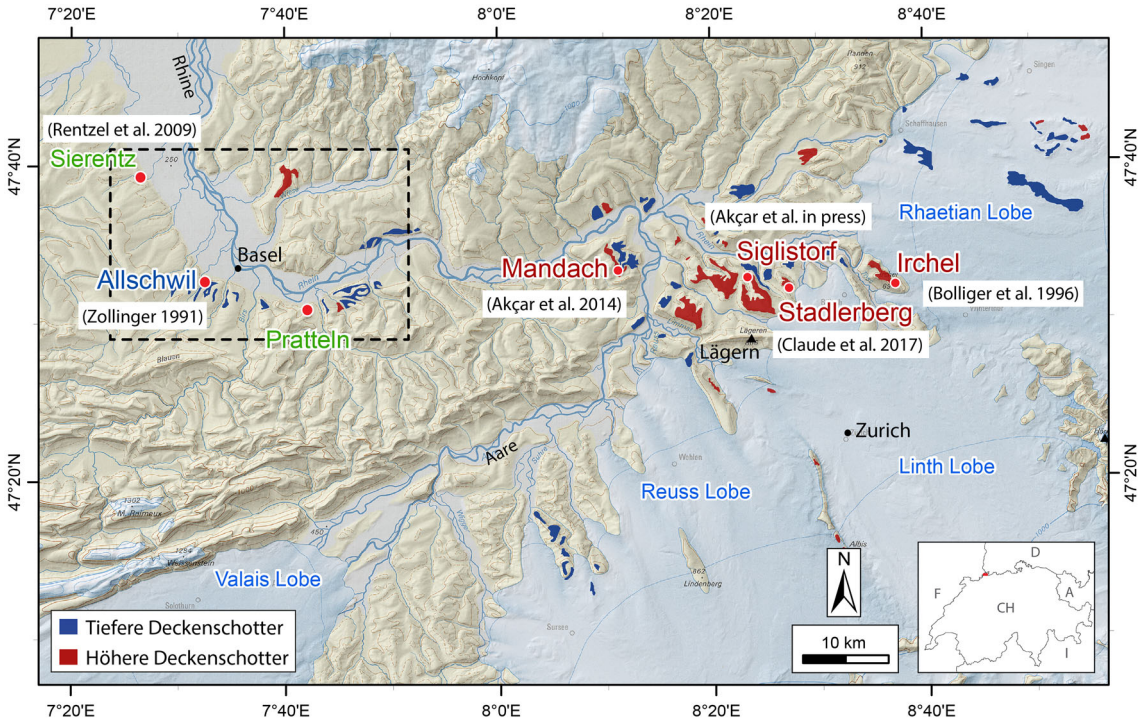

Fig. 1 Extension of the Valais, Reuss, Linth and Rhaetian Lobes during the Last Glacial Maximum (from Bini et al. 2009) and location of the Quaternary sites Sierentz, Allschwil, Mandach, Siglistorf, Stadlerberg and Irchel from which chronologies are available. In *blue* and *red* the distribution of the Tiefere and Höhere Swiss Deckenschotter in the northern Alpine Foreland are shown (© Federal Office of Topography, swisstopo, CH-3084 Wabern). The *dashed black square marks* the outline of Fig. 2

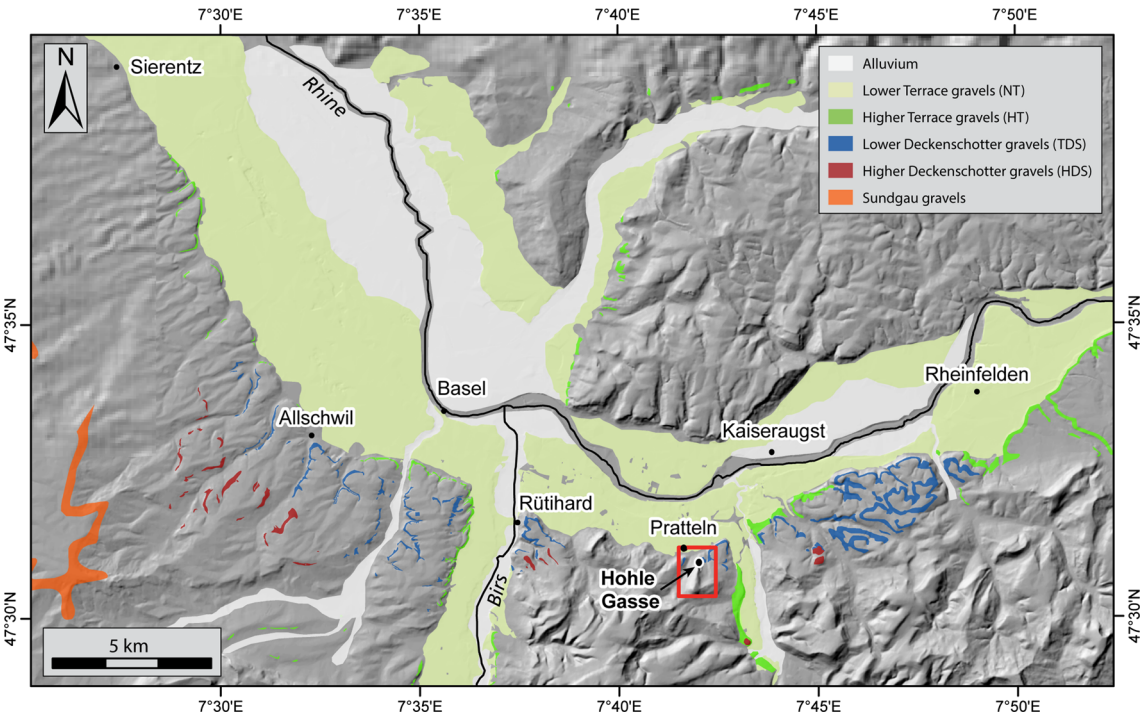

Fig. 2 Map with the Quaternary terrace units (NT, HT, TDS and HDS) of the Rhine River. In addition, the Sundgau gravels are shown, which are believed to have a Pliocene age based on biostratigraphic dating (Petit et al. 1996; Fejfar et al. 1998). The *red bold square* shows location of Fig. 4. (© Federal Office of Topography, swisstopo, CH-3084 Wabern)

magnetization (Zollinger 1991) and suggest that TDS accumulation may have occurred during an epoch older than the Brunhes epoch, hence older than 780 ka (Spell and McDougall 1992).

The younger Quaternary units HT are found tens of meters above NT units outside as well as inside overdeepened valleys (e.g. Penck and Brückner 1909). The overdeepened valleys contain thick sequences of till and lacustrine deposits (e.g. Schlüchter 1988/89; Graf and Müller 1999; Graf 2009; Dehnert et al. 2012; Buechi et al. 2017). In these valleys, a complex lithostratigraphy is encountered with valley fillings, nested into each other (Graf 2009; Preusser et al. 2010). The HT and NT deposits in the Alpine Foreland have been dated more frequently with different dating methods revealing minimum ages of gravel deposition between approximately 250–150 ka (e.g. Rentzel et al. 2009; Preusser et al. 2011; Dehnert et al. 2012; Lowick et al. 2015). Finally, the gravels of NT accumulated during the last glaciation of the Foreland, between 30 and 15 ka ago (Preusser et al. 2007; Kock et al. 2009a, b).

In this paper, we focus on the terrace gravels at Pratteln, Hohle Gasse (canton Basel-Landschaft, northwestern Switzerland) (Figs. 1, 2). The terrace deposits in this area were studied in detail by Du Pasquier (1891) and Frei (1912). Du Pasquier (1891) in his compilation of glaciofluvial gravels of northern Switzerland mapped them as HT. Frei (1912) and Bitterli-Brunner et al. (1984) however mapped the study area as TDS. A hand axe was found in 1974 by C. Hauser at this site and was attributed typologically to the Middlea Acheulean industry (d'Aujourd'hui 1977). Raw material analyses by J. Affolter (pers. comm., 1966) gave evidence that the hand axe was made of reworked Upper Jurassic flint from Eocene deposits near Lausen (canton Basel-Landschaft, some 8 km distance to the south east. The hand axe clearly shows traces of a displacement, indicating a complex taphonomic history of the artefact. In our study, we use sedimentological analyses such as clast fabric and petrography to infer the transport mechanism and depositional environment of the deposits and to deduce their provenance. Moreover, using cosmogenic ^{10}Be and ^{36}Cl depth-profile dating might help to evaluate the stratigraphical context of the deposits.

2 Geology of the study site Hohle Gasse

The study site Pratteln Hohle Gasse is situated in the Hochrhein Valley in Switzerland and is surrounded by the main geological features: the Jura Mountains to the south, the Black Forest to the north and the Upper Rhine Graben (URG) to the west. These three structures are lying on a major deep-seated ENE-WSW thrust fault (Permo-Carboniferous trough system), which was shown to be tectonically active during the Pleistocene (Schumacher 2002; Giamboni et al. 2004; Ustaszewski and Schmid 2007) (Fig. 3). Situated in the Tabular Jura, the location called Hohle Gasse ('hollow-way') leads from the historical centre of Pratteln up to Adlerberg (Figs. 2, 4). With an elevation of 296 m a.s.l., the village of Pratteln is located on a NT, whereas the Adlerberg consists of Jurassic limestone (Du Pasquier 1891; Frei 1912; Bitterli-Brunner et al. 1984) (Fig. 4). Profile 1, at an elevation of 333 m a.s.l., ca. 3 m deep, shows in its basal part the contact of limestone bedrock with the studied deposits (Fig. 5). Along this profile, samples were collected for dating with the cosmogenic nuclides ^{10}Be and ^{36}Cl. Based on the geological map, the Deckenschotter unit in this area has been mapped as a thin layer east and west of Hohle Gasse and which has not been mapped farther south of the study site (Bitterli-Brunner et al. 1984) (Figs. 2, 4). The near surroundings of the study site consist either of colluvium or slope debris (Fig. 4).

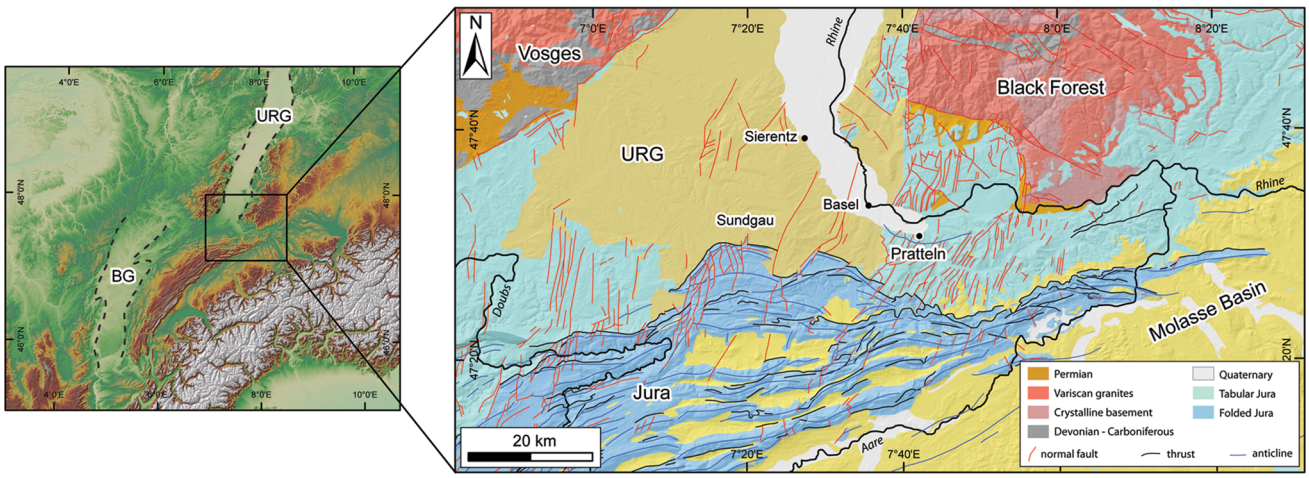

Fig. 3 Tectonic map of the study area and surroundings (after Spicher 1980). *URG* Upper Rhine Graben, *BG* Bresse Graben

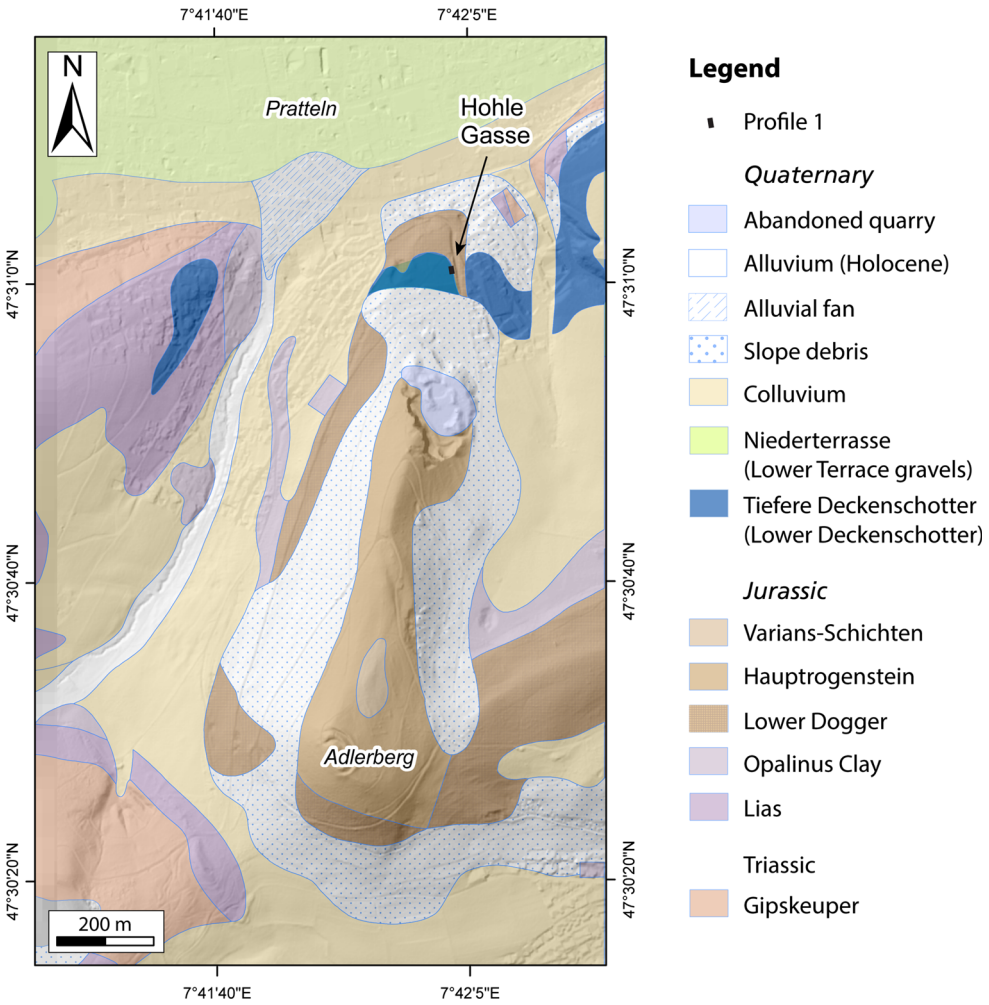

Fig. 4 Geological map of the study area Hohle Gasse based on Geologischer Atlas der Schweiz 1:25,000 (Bitterli-Brunner et al. 1984; © Federal Office of Topography, swisstopo, CH-3084 Wabern)

3 Methodology

3.1 Clast fabric and petrography

We analysed the lithostratigraphy of the sequence in detail in an effort to reconstruct the provenance of the sediments and to identify the transport mechanisms. Approximately 250 clasts were collected from profile 1 using a bucket (Fig. 5b). This allows sampling without any visual preference (after Schlüchter 1989; Graf 1993). Afterwards, the clasts were sieved to the gravel fraction (16–63 mm) and the following lithological classes were differentiated: (1) dark grey Alpine limestone, (2) light grey limestone, (3) Jurassic limestone, (4) siliceous limestone, (5) dolomite, (6) vein quartz, (7) quartzite, (8) sandstone, (9) radiolarite, (10) chert/hornstone and (11) magmatic and metamorphic crystalline rocks. Furthermore, special note was taken on the presence of key lithologies, which were transported to the Foreland with a glacier and indicate a limited source area (Hantke 1980; Graf 1993).

We also determined roundness and flattening indices on approximately 100 clasts of the gravel fraction from the same lithology, here vein quartz, for characterization purposes. No significant results will emerge when determining morphometric values on mixed lithologies as the various rock types have different transport resistances. The roundness (Z_i) and flattening (A_i) indices are calculated using the following formulas:

$$Z_i = \frac{2r_1}{L} \times 1000, \quad \text{(a))}$$

$$A_i = \frac{L + l}{2E} \times 100, \quad \text{(b),)}$$

where L is the length of the clast, $2r_1$ the smallest radius of curvature, l the width and E the thickness of the clast (Cailleux 1947; Schlüchter 1989). The calculated individual Z_i and A_i values are plotted in a histogram in value groups from 1 to 50, 51 to 100, 101 to 150, etc. High Z_i values correspond to rounded clasts whereas low Z_i values represent subangular clasts. High A_i values illustrate flat clasts. Then, the roundness Md(Z_i) and flattening Md(A_i) indices are determined by calculating the median and can be used for comparisons with values from other Quaternary unconsolidated deposits (Sneed and Folk 1958; Schlüchter 1989; Benn and Ballantyne 1994).

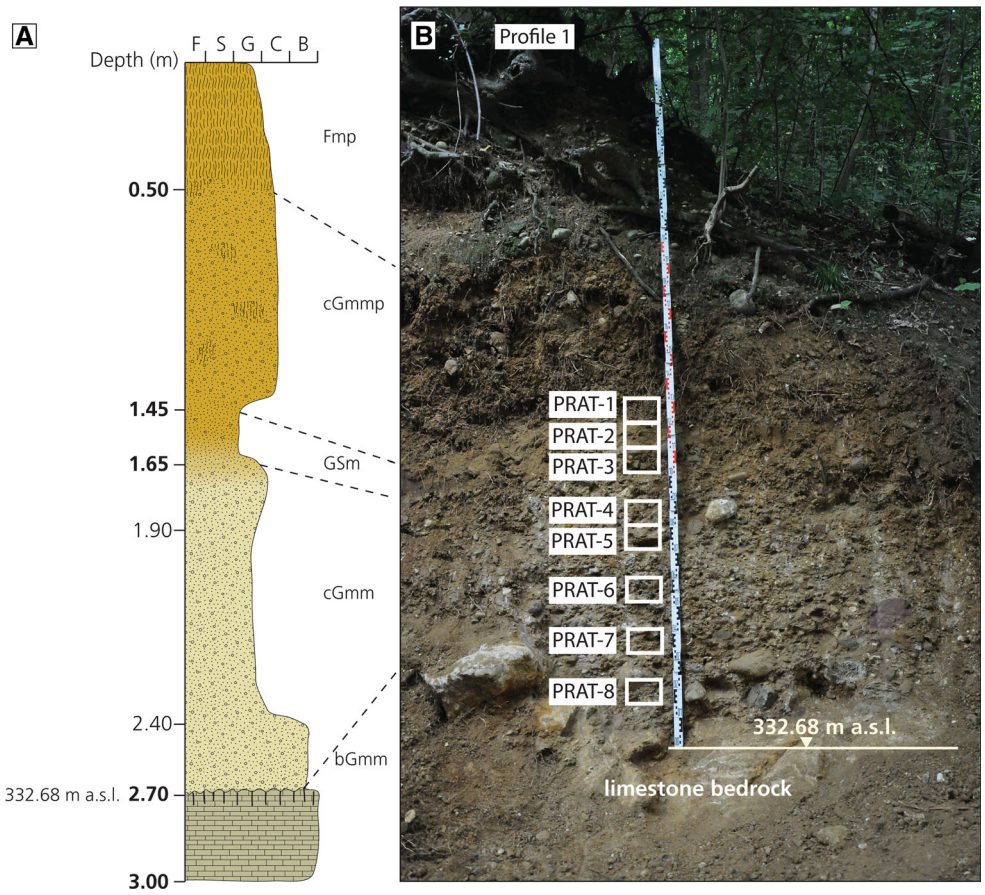

Fig. 5 **a** Stratigraphic column of the profile. The lithofacies code is based on Miall (1978) and Keller (1996). **b** Field photograph illustrating the sampled outcrop for depth-profile dating with ^{10}Be and ^{36}Cl

3.2 Geochronology

3.2.1 Dating with cosmogenic ^{10}Be and ^{36}Cl

Cosmogenic nuclides are produced through secondary cosmic ray particles in minerals of rocks and sediment within about 2 m of the Earth's surface (Gosse and Phillips 2001). By measuring their concentration, it can be determined how long a rock or sediment has been exposed to cosmic rays (Lal 1991; Gosse and Phillips 2001). Depth-profile dating is based on the fact that the build-up of cosmogenic nuclides decreases with depth following known physical principles (Gosse and Phillips 2001). For this method to be successful, it is essential to sample geological units in an artificial outcrop (e.g. road cut or gravel pit) with a flat-topped landform (e.g. Akçar et al. 2014; Claude et al. 2017). Repka et al. (1997) were the first to apply this method on fluvial terraces of the Fremont River in Utah.

At Hohle Gasse in Pratteln, a new 2 m long trench was opened by archaeologists, which gave access to fresh sampling material (Fig. 5b). Along a vertical profile of approximately 3 m, eight sediment samples with a thickness of 10 cm were collected for dating purposes with ^{10}Be and ^{36}Cl (Fig. 5b; Tables 1, 2). All samples were sieved to the sand fraction between 250 and 400 µm and were further processed in the Surface Exposure Dating Laboratory of the Institute of Geological Sciences at the University of Bern using nuclide specific procedures.

Cosmogenic ^{10}Be is mainly produced through spallation reactions, only a few percent are produced through muon interactions (Gosse and Phillips 2001). For the ^{10}Be samples, the lab protocol described in Akçar et al. (2012a) was followed. The ^{10}Be/^{9}Be measurements were then carried out at the accelerator mass spectrometry (AMS) at the ETH tandem facility in Zurich (Christl et al. 2013). The long-term weighted average ^{10}Be/^{9}Be ratio of $(2.26 \pm 0.32) \times 10^{-15}$ was used for full process blank correction.

A minimum ^{10}Be depth-profile age was modelled using Monte Carlo simulations in MATLAB® developed by Hidy et al. (2010; available online at http://geochronology.earthsciences.dal.ca/downloads-models.html) based on exposure age, erosion rate and inheritance. Figure 6 shows the Matlab interface with the input parameters for the age modelling. No correction factor was applied for topographic shielding and cover and thus the default value 1 was utilised as input. The ^{10}Be half-life with a value of 1.387 ± 0.012 Ma was used (Chmeleff et al. 2010;

Table 1 Sample information and cosmogenic ^{10}Be of the sediment samples from Hohle Gasse, Pratteln (N 47.5158, E 7.7002, 335 m a.s.l.)

Sample name	Sample depth (cm)	Quartz dissolved (g)	^{9}Be spike (mg)	^{10}Be/^{9}Be ($\times 10^{-14}$)	Relative uncertainty (%)	^{10}Be concentration (10^4 atoms/g)
PRAT-1	1.45	50.0077	0.1388	15.54	5.5	2.84 ± 0.16
PRAT-2	1.55	49.9186	0.1387	13.42	6.5	2.45 ± 0.16
PRAT-3	1.65	47.8717	0.1388	14.61	5.6	2.78 ± 0.16
PRAT-4	1.85	51.1690	0.1351	14.43	5.8	2.50 ± 0.15
PRAT-5	1.95	40.6884	0.1391	10.64	6.4	2.37 ± 0.16
PRAT-6	2.15	49.8949	0.1388	12.77	5.8	2.33 ± 0.14
PRAT-7	2.35	44.6941	0.1392	12.25	6.6	2.50 ± 0.17

AMS measurement errors are at 1σ level, including the statistical (counting) error and the error due to normalization of the standards and blanks. The error weighted average ^{10}Be/^{9}Be full process blank ratio is (2.26 ± 0.32) × 10^{-15}. Reported blank ratio and concentration are referenced to S2007N (Kubik and Christl 2010)

Table 2 Sample information and cosmogenic ^{36}Cl data of the sediment samples from Hohle Gasse, Pratteln (N 47.5158, E 7.7002, 335 m a.s.l.)

Sample name	Sample depth (cm)	Rock dissolved (g)	^{35}Cl spike (mg)	Cl concentration in rock (ppm)	^{36}Cl concentration (10^4 atoms/g)
PRAT-1	1.45	52.74	2.4173	47.2 ± 0.1	1.38 ± 0.19
PRAT-2	1.55	51.66	2.4183	45.8 ± 0.4	1.10 ± 0.13
PRAT-3	1.65	52.21	2.4183	46.9 ± 0.7	1.94 ± 0.43
PRAT-4	1.85	50.92	2.4144	46.3 ± 0.1	2.45 ± 0.23
PRAT-5	1.95	49.40	2.4113	38.8 ± 0.4	1.21 ± 0.14
PRAT-6	2.15	50.76	2.4185	39.6 ± 0.1	1.13 ± 0.15
PRAT-7	2.35	51.08	2.4149	46.5 ± 0.1	1.32 ± 0.16
PRAT-8	2.55	51.16	2.4161	42.7 ± 0.3	0.69 ± 0.09

AMS measurement errors are at 1σ level, including the statistical (counting) error and the error due to normalization of the standards and blanks

Korschinek et al. 2010). The ^{10}Be production rate was locally scaled with the Lal (1991) and Stone (2000) scheme using a reference production rate due to spallation of 3.93 ± 0.19 at/g/a (Northeastern North America production rate calibration dataset; Balco et al. 2009; CRONUS-Earth calculator update from v. 2.1 to v. 2.2 published by Balco in October 2013 after Balco et al. 2008; http://hess.ess.washington.edu/). Accordingly, a site specific spallogenic production rate of 4.93 ± 0.15 at/g/a resulted. Calculation of the muonic production was fit to a depth of 3 m. We assessed a bulk density of 1.8 ± 0.3 g/cm^3 (Manger 1963) for the sediment samples and assumed that it remains constant with depth within the range.

The inheritance of the depth profile is well constrained by the concentration of the lowermost sample, ca. 23,000 atoms/g (Table 1). From palaeomagnetic studies in an abandoned TDS quarry near Allschwil it is assumed that TDS deposits are older than 780 ka. Thus, we used as input a mean value of 1 Ma for the age and gave an error of 1 Ma. The erosion rate can be constrained by rates obtained from catchment-wide denudation rates calculated in the Alpine Foreland (e.g. Wittmann et al. 2007; Norton et al. 2008). Although, these denudation rates are probably higher as drainage basins erode in general more quickly than outcrops (Portenga and Bierman 2011). Furthermore, values for the erosion rates can be compared to the values from other studies using depth-profile dating: e.g. 5 cm/ka for the HDS Deckenschotter outcrop Stadlerberg in the Swiss Alpine Foreland (Claude et al. 2017), 3 ± 1 cm/ka for alluvial terraces in the French Western Alps (Brocard et al. 2003) and 3 cm/ka for alluvial terraces in southeastern France (Siame et al. 2004). Hence, we applied a mean value of 5 ± 5 cm/ka as input parameter. In addition, the Quaternary deposits in the area of the Sundgau Midlands, west of Basel show ca. 20 m thick loess sequences on top (Rentzel et al. 2009). Furthermore, an idea on the minimum value for the net erosion can be gained from the topography as well. In this case the area above the sampling site (335 m a.s.l.) is not a plateau but a gentle slope up to the bedrock of the Hauptrogenstein Formation, where the abandoned quarry is at an elevation of ca. 380 m a.s.l. (Fig. 4). This height difference of 40 m gives the maximum amount of net erosion. Therefore, the boundaries are set between 20 and 40 m (Fig. 6). We applied an attenuation length of 160 ± 5 g/cm^2 for sample shielding at depth (Dunne et al. 1999). Finally, to model an age we ran

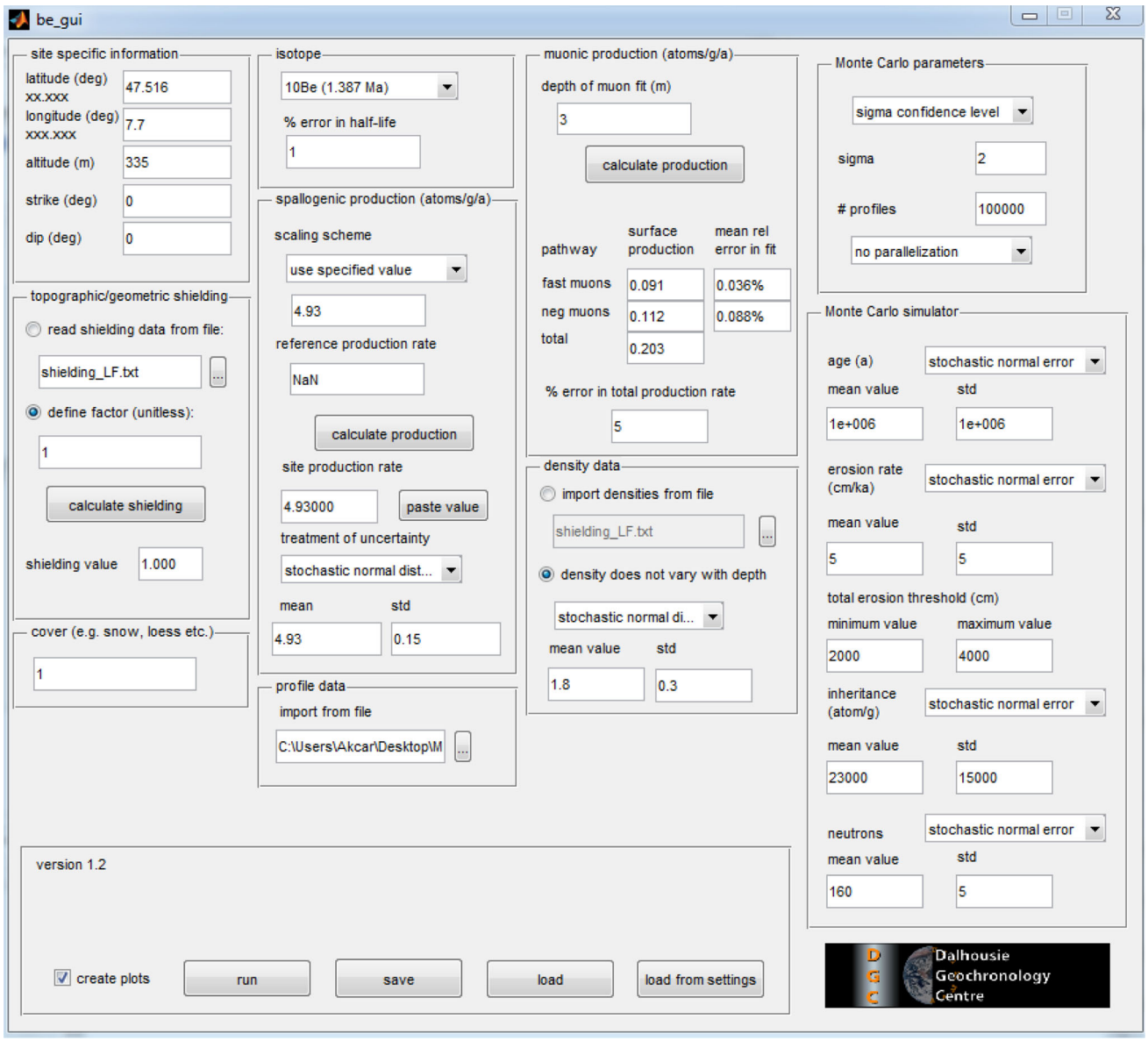

Fig. 6 Snapshot of the Matlab user interface of the Hidy et al. (2010) code for modelling a ^{10}Be age

the code for 100,000 profiles using a 2σ confidence window.

^{36}Cl differs from ^{10}Be as it is produced by three different reactions: (1) spallation of the elements Ca, K, Ti and Fe. This reaction is most important at the surface and decreases with depth; (2) slow negative muon capture by ^{40}Ca and ^{39}K, which is predominant at greater depths; (3) low-energy neutron capture (thermal and epithermal) by ^{35}Cl prevailing in the upper few meters below the ground (e.g. Zreda and Phillips 1994; Gosse and Phillips 2001). Sample preparation for ^{36}Cl is described in detail in Akçar et al. (2012b) and is based on isotope dilution (Stone et al. 1996; Elmore et al. 1997; Ivy-Ochs et al. 2004; Desilets et al. 2006). Total Cl and ^{36}Cl were measured on the same target at the AMS facility in Zurich. Furthermore, major element concentrations as well as analysis of uranium (U), thorium (Th), boron (B), gadolinium (Gd) and samarium (Sm) were performed at XRAL, Ontario, Canada (Table 3). The aliquots were taken from the leached samples after sieving. These major and trace elements were used to calculate the production rates and amount of neutrons available for production of ^{36}Cl through neutron capture (Alfimov and Ivy-Ochs 2009).

4 Results

4.1 Clast petrography and fabric

The studied outcrop has a massive fabric, is poorly-sorted and matrix-supported with an average grain size of 4 cm ranging

Table 3 Major and trace element data (determined by XRAL, Ontario, Canada) of the samples from Hohle Gasse, Pratteln

Sample name	SiO_2 (wt%)	Al_2O_3 (wt%)	Fe_2O_3 (wt%)	MnO (wt%)	MgO (wt%)	CaO (wt%)	Na_2O (wt%)	K_2O (wt%)	TiO_2 (wt%)	P_2O_5 (wt%)	Sm (ppm)	Gd (ppm)	U (ppm)	Th (ppm)
PRAT-1	46.71	1.74	0.27	0.00	0.07	0.08	0.00	5.86	0.03	0.01	0.80	0.76	0.69	2.20
PRAT-2	47.09	1.65	0.29	0.00	0.07	0.08	0.00	5.38	0.03	0.01	0.80	0.81	0.70	2.30
PRAT-3	47.53	1.58	0.30	0.00	0.07	0.04	0.00	4.89	0.04	0.01	0.80	0.85	0.69	2.30
PRAT-4	47.84	1.51	0.30	0.00	0.07	0.08	0.00	4.40	0.04	0.01	0.90	0.88	0.81	2.50
PRAT-5	47.69	1.60	0.32	0.00	0.07	0.08	0.00	4.40	0.05	0.01	0.90	0.86	0.8	2.50
PRAT-6	46.77	1.74	0.38	0.00	0.07	0.08	0.00	5.38	0.05	0.01	0.90	0.90	0.85	2.90
PRAT-7	45.96	1.92	0.37	0.01	0.08	0.08	0.00	6.35	0.05	0.01	0.90	0.86	0.84	2.80
PRAT-8	46.55	1.63	0.76	0.00	0.07	0.08	0.00	4.89	0.05	0.03	0.90	0.95	0.83	2.70
Average	47.02	1.67	0.37	0.00	0.07	0.07	0.00	5.19	0.04	0.01	0.86	0.86	0.78	2.53

up to a maximum of ca. 25 cm. Clasts are subrounded to rounded in shape, and only a minority are subangular. Imbrication is absent and thus no palaeocurrent direction could be determined. The stratigraphic section shows a crude fining-upward trend between a depth of 2.70 and 1.65 m with largest clast sizes of up to ca. 25 cm at the contact with the bedrock (Fig. 5). However, sporadically isolated larger clasts with a size of 12 cm occur. The beige-brownish matrix consists of sand, silt and clay. At a depth of 1.65–1.45 m, a sand-rich layer of orange-brownish colour is observed and overlies an undulatory boundary (Fig. 5). Few clasts are found in this sand layer. The upper part of the profile (1.45–0.5 m) shows matrix-supported clasts with an average clast size of 12 cm. Furthermore, this layer has been overprinted by modern soil formation. Half a meter of soil tops the profile and tree roots are penetrating down to its base (Fig. 5).

Given that the profile is only 3 m thick and is affected by pedogenesis in the upper part, petrographic analyses of clasts were performed between 2.70 and 1.65 m (Fig. 7a, b, d). Clasts of crystalline lithologies as well as sandstones are often weathered and at times break apart. All other lithologies are still intact and have no fractures or cracks. Numerous clasts are surrounded by a brown weathering rim. In addition, holes resulting from dissolved clasts are frequent. Clast counts show that the majority consists of chert (27%) followed by sandstone constituents (23%) (Fig. 7c). The relative abundance of vein quartz (18%), quartzites (17%) and magmatic and metamorphic crystalline lithologies (16%) is more or less the same. The contribution of radiolarite clasts is only 1%. Crystalline lithologies are made of red granite, gneiss and mica schist. No key lithologies, which would point to transport by a specific palaeoglacier system and hence indicate a limited source area (e.g. Hantke 1980; Graf 1993), were identified.

Together with the petrographic investigations, clast shape enables to identify the provenance of the gravel deposit. It is possible to differentiate between a provenance from Miocene Molasse (reworked) and a provenance directly from the Alps ('fresh'). The results from clast morphometric analyses are shown in Fig. 8a, b. Roundness indices (Z_i) have values between 150 and 600 and a median $Md(Z_i)$ of 333. The histogram shows a multimodal distribution with a first mode between 200 and 250, a second, main mode between 350 and 400 and a third minor mode between 500 and 550. The flattening indices (A_i) range from 100 to 350 with a median $Md(A_i)$ of 182.

Field observation and geochemical analysis ($CaCO_3$ is ca. 0%; Table 3) indicate that the whole profile is completely decalcified and all carbonate components are thus absent. The polished section in Fig. 7d shows for instance granitic gravels with porous structure (alteration of micas) or cherts with decalcified veins.

4.2 Cosmogenic nuclide dating

Measured ^{10}Be concentrations with uncertainties are shown in Table 1. ^{10}Be concentrations of the sediment samples range from $(2.33 \pm 0.14) \times 10^4$ atoms/g for PRAT-6 to $(2.84 \pm 0.16) \times 10^4$ atoms/g for PRAT-1. The contribution of the full process blank (2.26×10^{-15}) correction is less than 3%. ^{10}Be concentrations plotted against depth are illustrated in Fig. 9. A slight decrease with depth is recognizable.

Cl and ^{36}Cl concentrations with uncertainties are shown in Table 2. Table 3 shows major element as well as samarium, gadolinium, uranium and thorium concentrations. ^{36}Cl concentrations have values between $(2.45 \pm 0.23) \times 10^4$ atoms/g and $(0.69 \pm 0.09) \times 10^4$ atoms/g for the sediment samples PRAT-4 and PRAT-8 (Table 2). Compared to ^{10}Be, ^{36}Cl concentrations show a similar decrease with depth (Fig. 9). In case of ^{36}Cl, the chemical composition of the surrounding sediment is crucial to quantify the depth-dependent production through thermal neutron capture. Total Cl concentrations for the

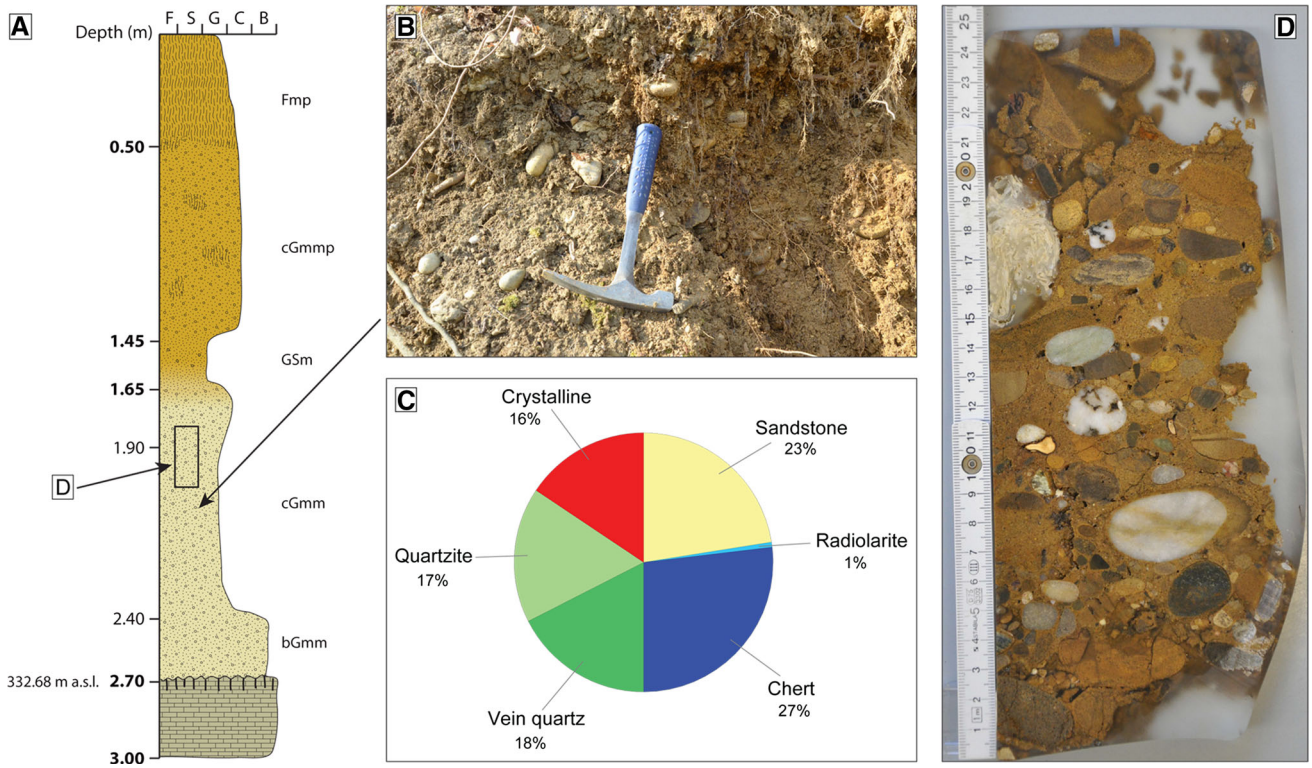

Fig. 7 **a** Stratigraphic column of the sampled profile. **b** Field photograph where clast petrography was performed. **c** Results of clast petrography. **d** Polished section of an undisturbed block of sediment impregnated with resin showing a decalcified and strongly altered gravel. The exact location is shown by the *black square* in **a**

eight sediment samples vary between 39 and 47 ppm indicating that the production of ^{36}Cl by neutron capture in the subsurface is non-negligible (Table 2). Sample ratios were corrected for a full process blank of 2.2×10^{-14}. In comparison to the measured ratios this comprised a blank correction of more than 50% for most samples. ^{36}Cl concentrations are reported here, but no age was calculated because of this inordinate blank correction.

The output of the ^{10}Be age modelling is given in Table 4 and frequency distributions together with χ^2 values of exposure age, erosion rate and inheritance are shown in Fig. 10. The best fit through the ^{10}Be data points is illustrated in Fig. 11. The single red line in Fig. 11a is the best fit depth profile resulting from the modelling. The numerous red lines in Fig. 11b shows the resulting 2σ solution space. The Monte Carlo simulations for ^{10}Be resulted in a modal depth-profile age of 270^{+830}_{-190} ka for a modal erosion rate of $8.9^{+17.7}_{-5.5}$ cm/ka and an inheritance of $14,000^{+13,000}_{-11,000}$ atoms/g (Table 4). Since the modal values are similar to the mean and median values generated by the simulation, the errors of the modal values are given by the minimum and maximum values. Lowest χ^2 values of 235 ka for the age, 18,000 atoms/g for the inheritance and 10.3 cm/ka for the top erosion rate resulted from the best fit of the modelling (Table 4).

5 Discussion

5.1 Sedimentology of the deposits at Hohle Gasse in Pratteln

Studying the clast fabric in the profile reveals indications on the transport mechanisms of the sediments (e.g. Cailleux 1947; Sneed and Folk 1958; Boulton 1978; Benn and Ballantyne 1994; Lukas et al. 2013). Data about the clast shape allow quantifying whether the accumulated material at the sampling site comprises reworked Miocene Molasse accumulated in the Alpine Foreland (round shape) or rather fresh erosional products from the Alps (subangular shape) (Du Pasquier 1891; Frei 1912). Clast shape can give an indication on the mechanism of transport (Cailleux 1947).

Detailed characterization of the sedimentary facies in the outcrop at Hohle Gasse made it possible to reconstruct the depositional environment. The matrix-supported fabric of the gravels in the lower part of profile 1 refer to bedload transport by high-concentrated flows, where the matrix consists of finer fractions sand, silt and clay (Miall 1996). The poorly-sorted, massive interval, containing large clasts from cobbles to boulders may have been deposited by a high-magnitude flood with a large amount of silt and clay in suspension (Siegenthaler and Huggenberger 1993).

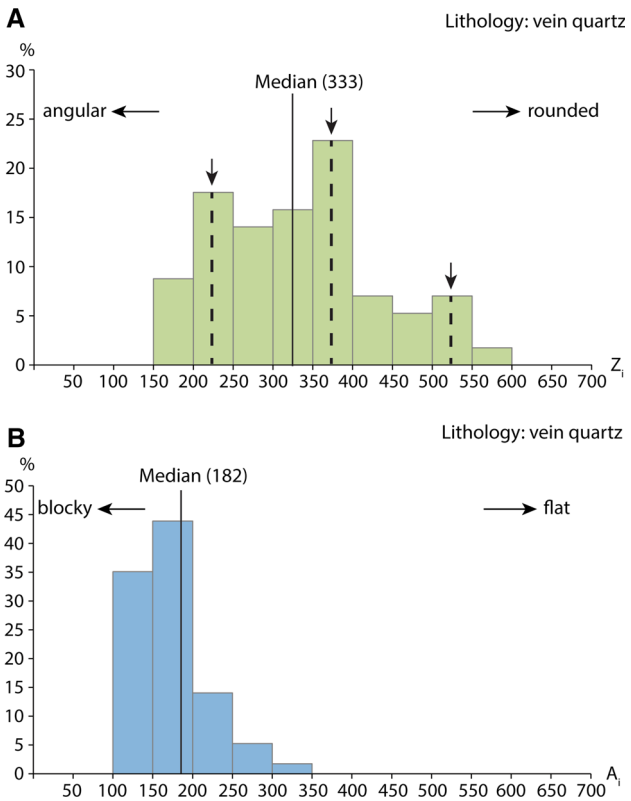

Fig. 8 Histograms illustrating the clast morphometry counting on vein quartz. **a** Roundness histogram, **b** flattening histogram

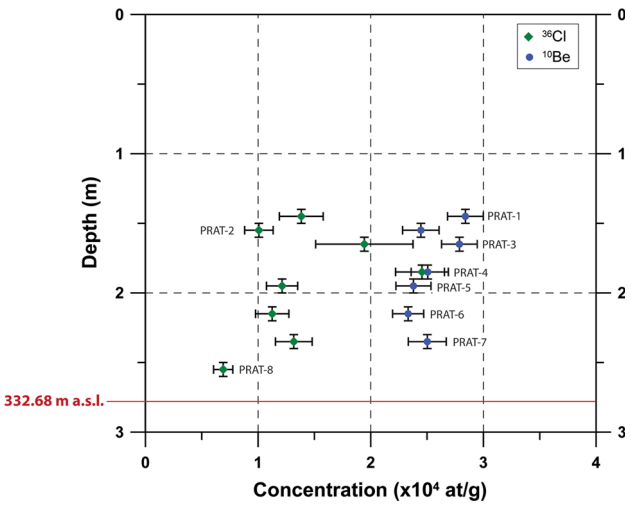

Fig. 9 Measured ^{10}Be and ^{36}Cl concentrations with 1σ uncertainties plotted against depth

However, parts of the silt and clay fraction can be alteration products (residual fraction) (Siegenthaler and Huggenberger 1993). Crude fining upward grading is generated from gravitational settling and the waning of the flood (Nemec and Steel 1984; Miall 1996). In addition, the sand-gravel mixture in the upper part of the profile shows changes in grain size, which can be related to variable current energy and differences in grain size supply (Heinz et al. 2003). In conclusion, the depositional environment of this sediment accumulation is linked to a braided river system where high-concentrated flows prevailed.

Analysis of clast morphometry supports transport and accumulation in a high-concentrated braided river system and provides additional information on the source area of the sediments. The median roundness index Md(Z_i) with a value of 333 is either correlated to a distal glaciofluvial environment, which extends between values of 100 and 330 or to a fluvial environment in a cold climate with Md(Z_i) values from 150 to 355 (Cailleux and Tricart 1959) (Fig. 8a). The first peak in the multimodal distribution with values between 200 and 250 is typical for a proximal glaciofluvial environment (e.g. Cailleux and Tricart 1959; Schlüchter 1976) (Fig. 8a). The second, dominant peak between 350 and 400 is characteristic for vein quartz clasts in a fluvial environment in a temperate climate (Cailleux and Tricart 1959) (Fig. 8a). Finally, the third peak from 500 to 550 characterises a typical fluvial environment (Schlüchter 1976) (Fig. 8a). Each peak in the multimodal distribution suggest one generation of transport: the first peak constitutes the youngest clasts whereas the third peak the oldest, that have been reworked once or twice (Schlüchter 1976). According to Schlüchter (1989) the flatness indices in general show little scatter in the distributions irrespective of the material sources. This variable has thus no power to infer the provenance of the material.

Our values can be compared to other studies. The Z_i values of the first peak agree with values from clast shape analysis on vein quartz at the HDS at Stadlerberg revealing a median roundness index Md(Z_i) of 272 (Claude et al. 2017). The depositional environment for these deposits was classified as proximal glaciofluvial. Values from the second peak are comparable to results obtained from crystalline clasts in 'Nagelfluh' (Molasse conglomerates) with Z_i values around 400 (Schlüchter 1976). Thus, the middle peak in the multimodal distribution most likely implicates better rounded, therefore, reworked clasts from the Miocene Molasse conglomerates. Finally, the third peak represents well-rounded clasts, which are either reworked from Molasse or from older Quaternary terrace deposits along the Rhine that had already incorporated clasts from the Molasse. In a previous study, Poser and Hövermann (1952) measured the clast morphometry on gravel deposits in Alpine valleys in the Zillertal (Austria). Clast roundness was determined on diorite clasts originating from glacial deposits in the glacier forefield, which had been transported downstream a distance between 2 and 4 km. In the roundness morphogram, the pure glacial character is no longer visible as the maximum peak is observed between Z_i values of 200 and 250 (Poser and Hövermann 1952). In addition, an increased occurrence of higher Z_i values is

Table 4 Results of age modelling with Matlab for ^{10}Be

	Age (ka)	Inheritance (104 atoms/g)	Erosion rate (cm/ka)
Mean	319	1.4	10.3
Median	303	1.4	10.0
Mode	268	1.4	8.9
Minimum χ^2	235	1.8	10.3
Maximum	1080	2.7	26.6
Minimum	84	0.3	3.4

Maximum and minimum values represent the 95% (2σ) confidence window for each parameter for the data

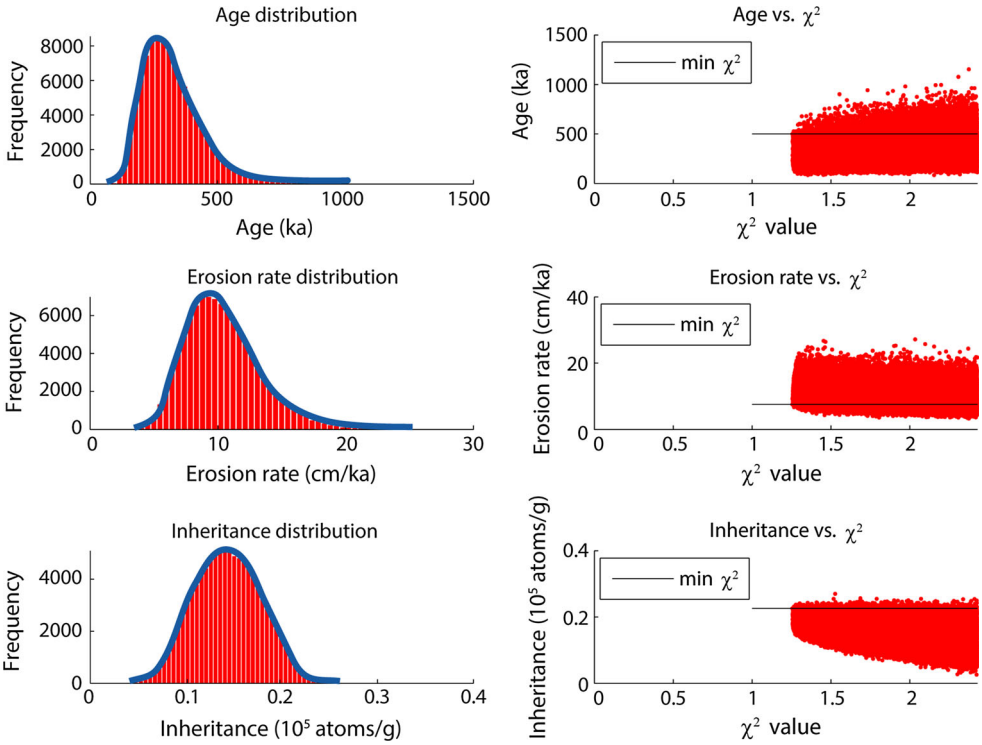

Fig. 10 Modal output of the Monte Carlo simulations showing frequency distributions and χ^2 values for age, erosion rate and inheritance

found with increasing distance from the forefield. Accordingly, the rather high roundness indices quantified at our study site Hohle Gasse imply a relatively long transport distance, more than a few tens of kilometres as well as a notable inclusion of reworked and redistributed material. Moreover, morphometric investigations were also performed in the NT gravels in the Rafzerfeld, in the Alpine Foreland (northern Switzerland) (Keller 1977). Alpine limestones from different gravel pits were analysed in order to allow a distinction between the different gravel bodies. The histograms showing the roundness indices showed multimodal distributions with three to four peaks resulting from reworking and redistribution, similar to our study. The median values vary between 289 and 389 (Keller 1977). Caution has to be taken however, since Alpine limestones are softer compared to the hard vein quartz, resulting probably in an increased roundness compared to the latter over the same distance. The tight distribution of the flatness morphogram with small values is an indication for a transport over a long distance as no flat clasts having higher A_i values are observed (Fig. 7b). This is in agreement with findings of Keller (1977) and Lukas et al. (2013). The latter authors studied clast shapes in glacial environments and revealed that clasts show more blocky and round forms when the environment changes from subglacial to distal fluvial, where patterns depend on clast lithologies as well. In conclusion, our clast morphometric data suggest that the gravel deposits at Hohle Gasse were deposited in a distal glaciofluvial environment. Some of the clasts (less than 20%) retain a clear glaciofluvial signal in their shape whereas the rest were at least reworked once.

Clast petrography investigations enable to determine the source area of sediment in an accumulation area (e.g. Dickinson 1988; Molinaroli and Basu 1993; Weltje and von Eynatten 2004). At the study site Hohle Gasse,

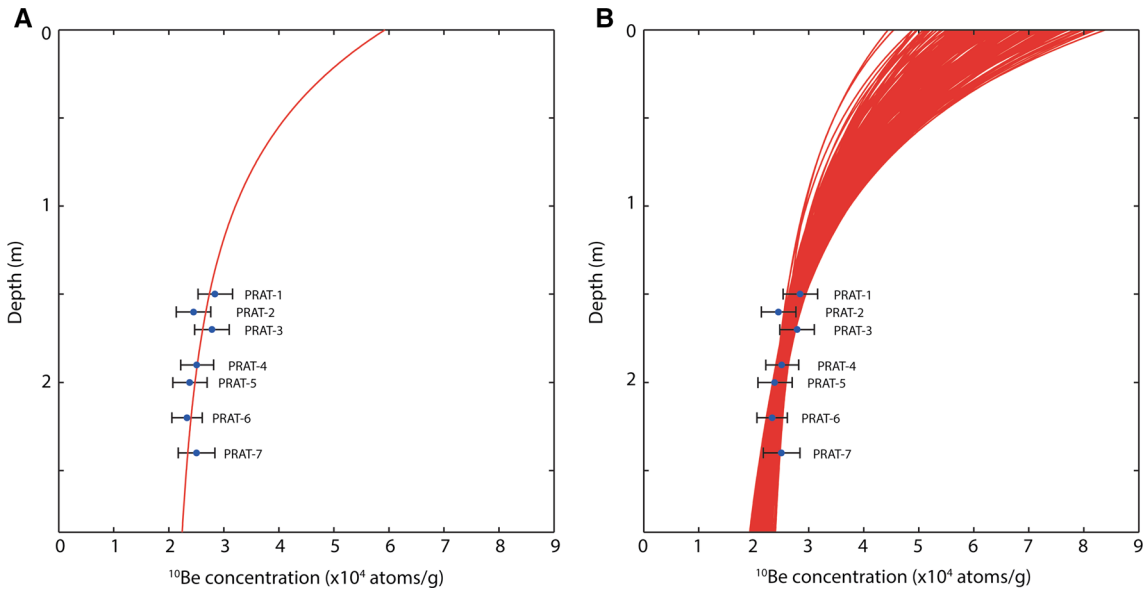

Fig. 11 Output of the Monte Carlo ^{10}Be depth-profile age simulation. **a** Illustration of the best fit through the seven data points for the 2σ confidence window. **b** Illustration of the resulting 2σ profile solution space

calcareous rocks such as limestone and dolomite constituents are not observed. One possibility for their absence could be related to weathering, which certainly plays an important role when the gravel layer is as thin as at it is here (Gerth and Becker-Haumann 2007). This would also explain the enrichment in lithologies with low erodibilities such as quartzite, vein quartz and chert lithotypes (Kühni and Pfiffner 2001). However, no molds are observed, which are usually found in intensely weathered deposits (e.g. Du Pasquier 1891; Frei 1912; Graf 1993). Another possibility for the absence of calcareous rocks could be that the majority of these deposits are reworked from older weathered sediments (Conradin 1991). In this case, the weak, non-resistant lithologies were completely destroyed during transport to the new accumulation area (*'Quarz-Restschotter'*, Schlüchter 1989). The vein quartz and sandstone lithologies do not reveal any information on the source area since they are abundant in the Molasse in the Alpine Foreland as well as in the Alps today (e.g. Richter 1930; Pavoni 1957; Matter 1964; Sartori et al. 2006). Quartzites from the greenschist facies in this setting, in contrast, would be a key clast for recycled Molasse (Schlunegger et al. 1998). The occurrence of this lithotype is negligible in the northern Alps. Yet, this clast type could have been derived trough glacial erosion in the Valais (Schlunegger et al. 1998). However, no greenschist-facies quartzite clasts were found. In addition, the location of Hohle Gasse, approximately 40 km downstream from the confluence of the Aare with the Rhine River, makes it impossible to distinguish whether the Western and/or Central Alps or the Eastern Alps contributed more material to the study site. Although weathered, it was still possible to discern the colour of the crystalline lithologies. Few red granitic clasts could be identified, which are a clear indicator of reworked Molasse (Matter 1964; Schlüchter 1989). Finally, no key lithologies were found, which would point to transport by a specific palaeoglacier system (e.g. Verrucano, Windgällen Porphyr, Taveyannaz Sandstone, Niesenbrekzie, Mont Blanc Granite or Arolla Gneis; after Hantke, 1980). In conclusion, clast petrography analyses did not provide any additional hint on the source area of the terrace gravels compared to the knowledge gained from clast morphometric investigations.

5.2 Timing of terrace formation and classification of the deposits

Our age from the cosmogenic ^{10}Be depth profile, 270^{+830}_{-190} ka, implies that we should reconsider today's classification of these gravels at Hohle Gasse in Pratteln as TDS on the geological map 1:25,000 (Bitterli-Brunner et al. 1984). So far, no numerical ages are yet available for TDS deposits in Switzerland, but based on paleomagnetic studies on the deposits in Allschwil they are expected to have an age of at least 780 ka (Zollinger 1991). The age of 270^{+830}_{-190} ka is in comparative agreement with a minimum OSL age of ca. 250 ka for the HT in Sierentz, which lies 25 km NNW of Hohle Gasse (Rentzel et al. 2009) (Fig. 1). Similarly, an OSL age of 260 ka was obtained from the lower part of a HT in the Lower Lech Valley at the original location where Quaternary stratigraphy was defined by

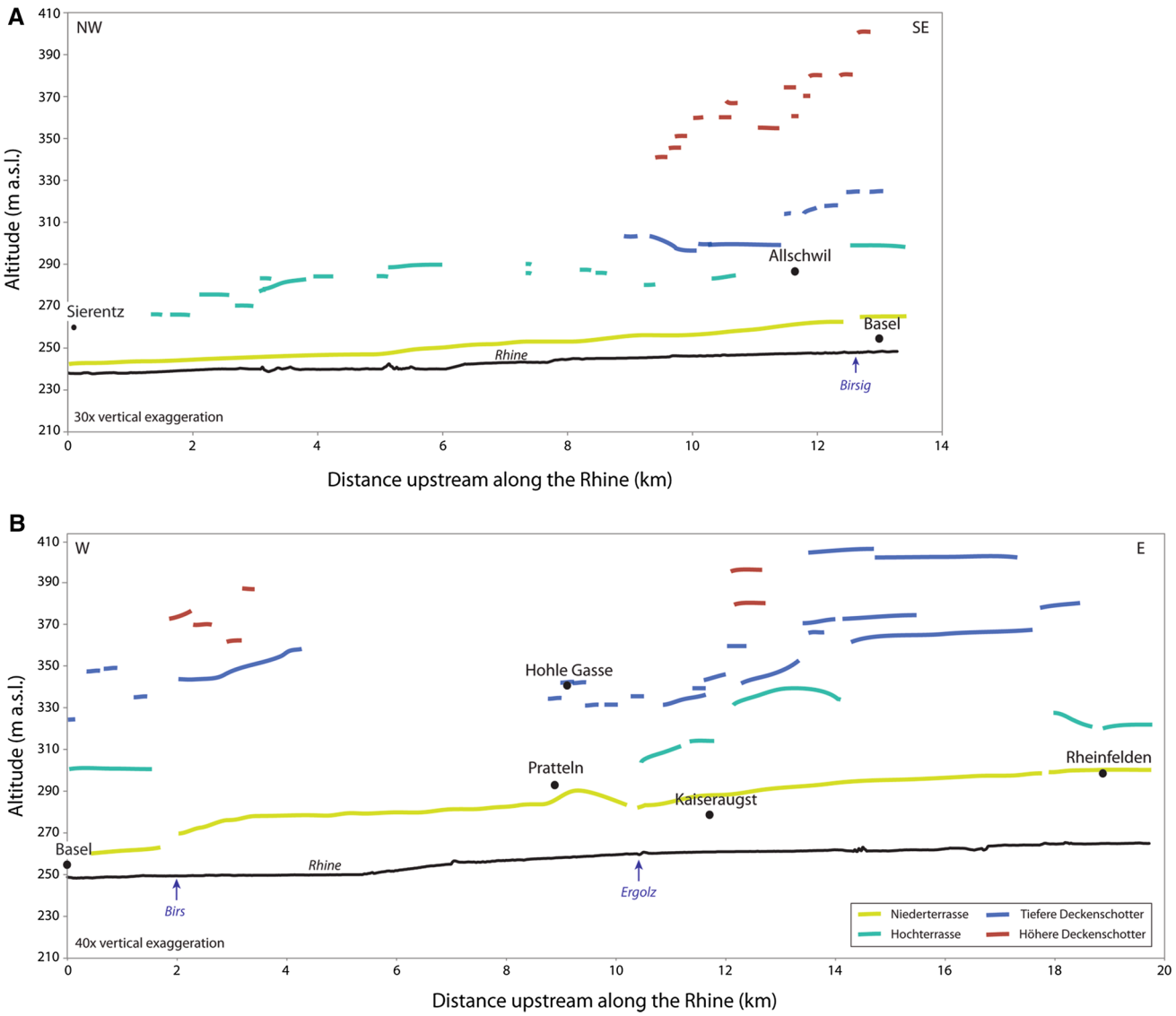

Fig. 12 Cross section along the River Rhine from Sierentz to Rheinfelden showing the distribution of the top surface of the Quaternary terraces: NT, HT, TDS and HDS (after Wittmann et al. 1970; Bitterli-Brunner et al. 1984; Heuberger et al. 2014 and Federal Office of Topography, swisstopo)

Penck and Brückner (1909) (Schielein et al. 2015). Our age from Hohle Gasse as well as the ones from the HT in Sierentz and Lower Lech Valley are ca. 100 to 150 ka older compared to other studies by Dehnert et al. (2010, 2012), Preusser et al. (2011), Lowick et al. (2015), Klasen et al. (2015) and Schielein et al. (2015) which dated the HT in the Swiss and German Alpine Foreland to MIS 6 (127–186 ka; Lisiecki and Raymo 2005). However, it was also shown that the deposits of HT cannot be correlated to only one glacial advance but represent multiple advances or even different glaciations instead (Gutzwiller 1894; Schlüchter 2004; Graf 2009; Keller and Krayss 2010; Ellwanger et al. 2011; Preusser et al. 2011; Schielein et al. 2015). Our results indicate that a major phase of aggradation was during MIS 8 (240–300 ka; Lisiecki and Raymo 2005). Accordingly, we propose to assign the deposits at Hohle Gasse in Pratteln to HT as previously mapped by Du Pasquier (1891).

It is comprehensible that these deposits were previously classified as TDS since a clear differentiation between TDS and HT based on sedimentological characteristics or elevation is difficult. The Quaternary deposits in Switzerland Deckenschotter, Hochterrasse and Niederterrasse have been extensively studied in the past (Du Pasquier 1891, Gutzwiller 1894; Penck and Brückner 1909; Frei 1912). Du Pasquier (1891) compared the deposits of HT with Deckenschotter sediments and pointed out that the latter show a higher degree of consolidation and cementation and a

strong decomposition of crystalline components. However, the strong cementation of Deckenschotter material only affects outcrops along exposed cliffs (Penck and Brückner 1909; Frei 1912). Recent collapses showed that parts which have not been exposed are rather weakly consolidated. Thus, the degree of cementation cannot strictly be used to differentiate between Deckenschotter and HT or NT. The fact that crystalline rocks in Deckenschotter sediments are strongly weathered was also observed by several authors (e.g. Penck and Brückner 1909; Frei 1912; Graf 1993; Claude et al. 2017). Furthermore, Du Pasquier (1891) revealed that numerous calcareous clasts have an altered surface indicating the occurrence of dissolving by groundwater and that 'clast holes' are common. In HT deposits in contrast, molds are rarely found. Frei (1912) pointed out though, that a few HT accumulations in the Hochrhein Valley also show 'clast holes'. Finally, considering the clast suites encountered in the material, Deckenschotter deposits contain more quartzite and other rocks from Molasse conglomerates than the younger accumulations of the HT and NT (Gutzwiller 1894; Penck and Brückner 1909). Since the studied outcrop at Hohle Gasse is completely decalcified, it is not feasible to compare the petrographic results with other studied Deckenschotter outcrops. Accordingly, the investigation of fabric of the deposits along with the morphometric and petrographic characteristics of the clasts alone does not help in clarifying the classification of the deposits at Hohle Gasse as HT or TDS.

In the past, it was assumed that different terrace levels accumulated during the four main glacial stages of the Alps and the Foreland and they were classified according to their elevation (Gutzwiller 1894; Du Pasquier 1891; Penck and Brückner 1909; Frei 1912; Hantke 1978; Haldimann et al. 1984; Verderber 1992; Graf 1993). Analysis of the top surface of the four different terrace units NT, HT, TDS and HDS indicates a general topographic dip along the Rhine between Rheinfelden and Sierentz (Fig. 10). Furthermore, the boundaries between the different terraces are not always clear especially between Basel and Rheinfelden, where both TDS and HDS units occur between 360 and 390 m a.s.l. (Kock 2008) (Fig. 12). Similarly, 3 km upstream from the study site Hohle Gasse, east of Kaiseraugst, HT deposits are outcropping at 330 m a.s.l., approximately at the same altitude as TDS sediments (Fig. 12). The comparison of elevations of different terraces is not always straightforward, especially if the former valley axis is unknown. Some deposits might occupy positions along the channel margin and are thus situated at a higher elevation compared to those in the centre of the channel axis with a lower elevation (Sinn 1972; Verderber 1992; Lempe 2012). Thus, based on the altitude of 335 m a.s.l. of Hohle Gasse it is also not possible to assign the terrace to either TDS or HT and only absolute dating allowed re-evaluating the stratigraphical context.

6 Conclusions

In this study, we focussed on deeply weathered terrace gravels at Hohle Gasse, 1 km SSE of Pratteln, in the northwestern Swiss Alpine Foreland where archaeologists opened a trench. From sedimentological analysis it is concluded that the gravels were deposited in a distal glaciofluvial environment in a high-concentrated braided river system. Only a minority of the analysed clasts retain a clear signal in their shape, the majority were reworked at least once.

Cosmogenic ^{10}Be depth-profile dating on seven sediment samples resulted in a minimum age of 270^{+830}_{-190} ka. A too high blank correction made it impossible to calculate an age from the ^{36}Cl concentrations. The ^{10}Be age reveals that the gravels cannot be classified as TDS. We suggest a classification to the HT level instead. In addition, our results show that at Hohle Gasse, distinguishing TDS and HT based on elevation is problematic and clast morphometry and petrography could as well not help to differentiate between TDS and HT. Our analyses further suggest that a major phase of aggradation occurred during MIS 8.

Acknowledgements We would like to thank the Laboratory of Ion Beam Physics, ETH Zurich, for the AMS measurements. This study was initiated and funded by Archäologie Baselland as well as the Swiss Federal Nuclear Safety Inspectorate ENSI (Project No. H-100898). We are grateful to Reto Marti and Jürg Sedlemeier for strong support and further thank Reto Jagher for comments about Quaternary Geology.

References

Akçar, N., Deline, P., Ivy-Ochs, S., Alfimov, V., Hajdas, I., Kubik, P. W., et al. (2012a). The AD 1717 rock avalanche deposits in the upper Ferret Valley (Italy): A dating approach with cosmogenic ^{10}Be. *Journal of Quaternary Science, 27*(4), 383–392.

Akçar, N., Ivy-Ochs, S., Alfimov, V., Claude, A., Graf, H. R., Dehnert, A., et al. (2014). The first major incision of the Swiss Deckenschotter landscape. *Swiss Journal of Geosciences, 107,* 337–347.

Akçar, N., Tikhomirov, D., Özkaymak, C., Ivy-Ochs, S., Alfimov, V., Sözbilir, H., et al. (2012b). 36Cl exposure dating of paleoearthquakes in the Eastern Mediterranean: First results from the western Anatolian Extensional Province, Manisa fault zone, Turkey. *Geological Society of America Bulletin, 124,* 1724–1735.

Akçar, N., Ivy-Ochs, S., Alfimov, V., Schlunegger, F., Claude, A., Reber, R., Christl, M., Vockenhuber, C., Dehnert, A., Rahn, M., Schlüchter, C. Isochron-burial dating of glaciofluvial deposits: Primary results from the Alps. Earth Surface Processes and Landforms (**in press**).

Alfimov, V., & Ivy-Ochs, S. (2009). How well do we understand the production of ^{36}Cl in limestone and dolomite? *Quaternary Geochronology, 4,* 462–474.

Balco, G., Briner, J., Finkel, R. C., Rayburn, J. A., Ridge, J. C., & Schaefer, J. M. (2009). Regional beryllium-10 production rate calibration for northeastern North America. *Quaternary Geochronology, 4,* 93–107.

Balco, G., Stone, J. O., Lifton, N. A., & Dunai, T. J. (2008). A complete and easily accessible means of calculating surface exposure ages or erosion rates from ^{10}Be and ^{26}Al measurements. *Quaternary Geochronology, 3,* 174–195.

Benn, D. I., & Ballantyne, C. K. (1994). Reconstructing the transport history of glacigenic sediments: A new approach based on the co-variance of clast form indices. *Sedimentary Geology, 91,* 215–227.

Bini, A., Buonchristiani, J.-F., Couterand, S., Ellwanger, D., Felber, M., Florineth, D., et al. (2009). *Switzerland during the Last Glacial Maximum (LGM), 1:500,000*. Wabern: Federal Office of Topography, swisstopo.

Bitterli-Brunner, P., Fischer, H., Herzog, P. (1984). Geologischer Atlas der Schweiz, 1:25,000, Blatt 1067 Arlesheim.

Bolliger, T., Fejfar, O., & Graf, H. R. (1996). Vorläufige Mitteilung über Funde von pliozänen Kleinsäugern aus den höheren Deckenschottern des Irchels (Kt. Zürich). *Eclogae Geologicae Helvetiae, 89*(3), 1043–1048.

Boulton, G. S. (1978). Boulder shapes and grain-size distributions of debris as indicators of transport paths through a glacier and till genesis. *Sedimentology, 25,* 773–799.

Brocard, G. Y., van der Beek, P. A., Bourlès, D. L., Siame, L. L., & Mugnier, J.-L. (2003). Long-term fluvial incision rates and postglacial river relaxation time in the French Western Alps from 10Be dating of alluvial terraces with assessment of inheritance, soil development and wind ablation effects. *Earth and Planetary Science Letters, 209,* 197–214.

Buechi, M., Lowick, S. E., & Anselmetti, F. S. (2017). Luminescence dating of glaciolacustrine silt in overdeepened basin fills beyond the last interglacial. *Quaternary Geochronology, 37,* 55–67.

Cailleux, A. (1947). L'indice émoussé; définition et première application. *Société Géologique de France, 13–14,* 251–252.

Cailleux, A., & Tricart, J. (1959). *Initiation à l'étude des sables et galets* (3 volumes: 369 pp., 194 pp, 303 pp.). Paris: Centre de Documentation Universitaire.

Chmeleff, J., von Blanckenburg, F., Kossert, K., & Jakob, D. (2010). Determination of the ^{10}Be half-life by multicollector ICP-MS and liquid scintillation counting. *Nuclear Instruments & Methods in Physics Research, Section B: Beam Interactions with Materials and Atoms, 268*(2), 192–199.

Christl, M., Vockenhuber, C., Kubik, P. W., Wacker, L., Lachner, J., Alfimov, V., et al. (2013). The ETH Zurich AMS facilities: Performance parameters and reference materials. *Nuclear Instruments & Methods in Physics Research, Section B: Beam Interactions with Materials and Atoms, 294,* 29–38.

Claude, A., Akçar, N., Ivy-Ochs, S., Schlunegger, F., Kubik, W. P., Dehnert, A., Kuhlemann, J., Rahn, M., Schlüchter, C. (2017). Timing of early Quaternary gravel accumulation in the Swiss Alpine Foreland. Geomorphology 276:71–85

Conradin, H. (1991). Pedologische und sedimentpetrographische Untersuchungen im Quartär der Nordschweiz. Ph.D. thesis, Swiss Federal Institute of Technology Zurich, Zurich, Switzerland, p. 255.

D'Aujourd'hui, R. (1977). Ein altpaläolithischer Faustkeil aus Pratteln BL. In L. Berger et al. (Hrsg.), Festschrift Elisabeth Schmid zu ihrem 65 Geburtstag (pp. 1–14). Basel: Regio Basiliensis.

Dehnert, A., Lowick, S. E., Preusser, F., Anselmetti, F. S., Drescher-Schneider, R., Graf, H. R., et al. (2012). Evolution of an overdeepened trough in the northern Alpine Foreland at Niederweningen, Switzerland. *Quaternary Science Reviews, 34,* 127–145.

Dehnert, A., Preusser, F., Kramers, J. D., Akçar, N., Kubik, P. W., Reber, R., et al. (2010). A multi-dating approach applied to proglacial sediments attributed to the Most Extensive Glaciation of the Swiss Alps. *Boreas, 39,* 620–632.

Desilets, D., Zreda, M., Almasi, P. F., & Elmore, D. (2006). Determination of cosmogenic Cl-36 in rocks by isotope dilution: Innovations, validation and error propagation. *Chemical Geology, 233*(3–4), 185–195.

Dickinson, W. R. (1988). Provenance and sediment dispersal in relation to paleotectonics and paleogeography of sedimentary basins. In K. L. Kleinspehn & C. Paola (Eds.), *New perspectives in basin analysis* (pp. 3–25). New York: Springer.

Du Pasquier, L. (1891). Über die Fluvioglacialen Ablagerungen der Nordschweiz (ausserhalb der inneren Moränenzone). Ph.D. dissertation, University of Zurich, Zurich, Switzerland, p. 128.

Dunne, J., Elmore, D., & Muzikar, P. (1999). Scaling factors for the rates of production of cosmogenic nuclides for geometric shielding and attenuation at depth on sloped surfaces. *Geomorphology, 27,* 3–11.

Ellwanger, D., Wielandt-Schuster, U., Franz, M., & Simon, T. (2011). The quaternary of the south German Alpine Foreland (Bodensee-Oberschwaben, Baden-Württemberg, South Germany). *Quaternary Science Journal, 60,* 306–328.

Elmore, D., Ma, X., Miller, T., Mueller, K., Perry, M., Rickey, F., et al. (1997). Status and plans for the PRIME Lab AMS facility. *Nuclear Instruments and Methods in Physics Research B: Beam Interactions with Materials and Atoms, 123,* 69–72.

Fejfar, O., Heinrich, W.-D., & Lindsay, E. H. (1998). Updating the Neogene rodent biochronology. *Mededelingen Nederlands Instituut voor Toegepaste Geowetenschappen, TNO, 60,* 533–554.

Frei, R. (1912). *Monographie des Schweizerischen Deckenschotters* (p. 182). Beiträge zur Geologischen Karte der Schweiz, N.F. 37.

Gerth, A., & Becker-Haumann, R. (2007). Sedimentuntersuchungen an unterpleistozänen Schmelzwasserablagerungen und Periglazialschottern im Riss-Iller-Gebiet, deutsches Alpenvorland. *E&G Quaternary Science Journal, 56*(3), 186–211.

Giamboni, M., Wetzel, A., Nivière, B., & Schumacher, M. (2004). Plio-Pleistocene folding in the southern Rhinegraben recorded by the evolution of the drainage network (Sundgau area; northwestern Switzerland and France). *Eclogae Geologicae Helvetiae, 97*(1), 17–31.

Gosse, J. C., & Phillips, F. M. (2001). Terrestrial in situ cosmogenic nuclides: Theory and application. *Quaternary Science Reviews, 20,* 1475–1560.

Graf, H.R. (1993). Die Deckenschotter der zentralen Nordschweiz. Ph.D. thesis, Swiss Federal Institute of Technology Zurich, Zurich, Switzerland, p. 150.

Graf, H.R. (2009). Stratigraphie von Mittel- und Spätpleistozän in der Nordschweiz. Beiträge zur Geologischen Karte der Schweiz N.F. 168. Wabern: Federal Office of Topography, swisstopo.

Graf, H. R., & Müller, B. (1999). Das Quartär: Die Epoche der Eiszeiten. In T. Bolliger (Ed.), *Geologie des Kantons Zürich* (pp. 71–95). Thun: Ott.

Gutzwiller, A. (1894). Diluvialbildungen der Umgebung von Basel. *Verhandlungen der Naturforschenden Gesellschaft in Basel, 10*(3), 512–690.

Haldimann, P., Naef, H., & Schmassmann, H. (1984). NTB 84-19: Fluviatile Erosions- und Akkumulationsformen als Indizien jungpleistozäner und holozäner Bewegungen in der Nordschweiz und angrenzenden Gebieten. Nagra Technischer Bericht.

Hantke, R. (1978). *Eiszeitalter. Die jüngste Erdgeschichte der Schweiz und ihrer Nachbargebiete. Band 1, Klima, Flora, Fauna, Mensch, Alt- und Mittel-Pleistozän, Vogesen, Schwarzwald, Schwäbische Alb, Adelegg* (p. 468). Thun: Ott Verlag.

Hantke, R. (1980). *Eiszeitalter. Die jüngste Erdgeschichte der Schweiz und ihrer Nachbargebiete. Band 2, Letzte Warmzeiten,*

Würm-Eiszeit, Eisabbau und Nacheiszeit der Alpen-Nordseite vom Rhein- zum Rhone-System (p. 703). Thun: Ott.

Heinz, J., Kleineidam, S., Teutsch, G., & Aigner, T. (2003). Heterogeneity patterns of Quaternary glaciofluvial gravel bodies (SW-Germany): Application to hydrogeology. *Sedimentary Geology, 158*(1–2), 1–23.

Heuberger, S., Büchi, M., & Naef, H. (2014). NAB 12-20: Drainage system and landscape evolution of northern Switzerland since the Late Miocene. Nagra Arbeitsbericht.

Hidy, A. J., Gosse, J. C., Pederson, J. L., Mattern, J. P., & Finkel, R. C. (2010). A geologically constrained Monte Carlo approach to modeling exposure ages from profiles of cosmogenic nuclides: An example from Lees Ferry. *Arizona. Geochemistry Geophysics Geosystems, 11,* 18.

Ivy-Ochs, S., Synal, H.-A., Roth, C., & Schaller, M. (2004). Initial results from isotope dilution for Cl and ^{36}Cl measurements at the PSI/ETH Zurich AMS facility. *Nuclear Instruments & Methods in Physics Research, Section B: Beam Interactions with Materials and Atoms, 223–224,* 623–627.

Keller, W. A. (1977). Die Rafzerfeldschotter und ihre Bedeutung für die Morphogenese des zürcherischen Hochrheingebietes. *Vierteljahrsschrift der Naturforschenden Gesellschaft in Zürich, 122*(3), 357–412.

Keller, B. (1996). Lithofazies-Codes für die Klassifikation von Lockergesteinen. *Mitteilungen der Schweizerischen Geologischen Gesellschaft für Boden- und Felsmechanik, 132,* 5–12.

Keller, O., & Krayss, E. (2010). Mittel- und spätpleistozäne Stratigraphie und Morphogenese in Schlüsselregionen der Nordschweiz. *E&G Quaternary Science Journal, 59*(1–2), 88–119.

Klasen, N., Fiebig, M., & Preusser, F. (2015). Applying luminescence methodology to key sites of Alpine glaciations in southern Germany. *Quaternary International*. doi:10.1016/j.quaint.2015.11.023.

Kock, S. (2008). Pleistocene terraces in the Hochrhein area - formation, age constraints and neotectonic implications. Ph.D. dissertation, University of Basel, Basel, Switzerland, p. 99.

Kock, S., Huggenberger, P., Preusser, F., Rentzel, P., & Wetzel, A. (2009a). Formation and evolution of the Lower Terrace of the Rhine River in the area of Basel. *Swiss Journal of Geosciences, 102,* 307–321.

Kock, S., Kramers, J. D., Preusser, F., & Wetzel, A. (2009b). Dating of Late Pleistocene terrace deposits of the River Rhine using Uranium series and luminescence methods: Potential and limitations. *Quaternary Geochronology, 4,* 363–373.

Korschinek, G., Bergmaier, A., Faestermann, T., Gerstmann, U. C., Knie, K., Rugel, G., et al. (2010). A new value for the half-life of Be-10 by heavy-ion elastic recoil detection and liquid scintillation counting. *Nuclear Instruments & Methods in Physics Research, Section B: Beam Interactions with Materials and Atoms, 268,* 187–191.

Kubik, P. W., & Christl, M. (2010). ^{10}Be and ^{26}Al measurements at the Zurich 6 MV Tandem AMS facility. *Nuclear Instruments & Methods in Physics Research, Section B: Beam Interactions with Materials and Atoms, 268,* 880–883.

Kühni, A., & Pfiffner, A. O. (2001). Drainage patterns and tectonic forcing: A model study for the Swiss Alps. *Basin Research, 13,* 169–197.

Lal, D. (1991). Cosmic ray labeling of erosion surfaces: In situ nuclide production rates and erosion models. *Earth and Planetary Science Letters, 104,* 424–439.

Lempe, B. (2012). Die geologischen Verhältnisse auf der GK25 Blatt Nr. 8027 Memmingen unter besonderer Berücksichtigung der Verwitterungserscheinungen in pleistozänen Schmelzwasserschottern und deren Einfluss auf ihre bautechnischen Eigenschaften. Entwicklung einer Verwitterungsklassifizierung. Ph.D. dissertation, Technical University of Munich, Munich, Germany, p. 376.

Lisiecki, L. E., & Raymo, M. E. (2005). A Pliocene-Pleistocene stack of 57 globally distributed benthic δ^{18}O records. *Paleoceanography, 20,* 1–17.

Lowick, S. E., Buechi, M. W., Gaar, D., Graf, H. R., & Preusser, F. (2015). Luminescence dating of Middle Pleistocene proglacial deposits from northern Switzerland: Methodological aspects and stratigraphical conclusions. *Boreas, 44*(3), 459–482.

Lukas, S., Benn, D. I., Boston, C. M., Brook, M., Coray, S., Evans, D. J., et al. (2013). Clast shape analysis and clast transport paths in glacial environments: A critical review of methods and the role of lithology. *Earth-Science Reviews, 121,* 96–116.

Manger, G.E. (1963). Porosity and bulk density of sedimentary rocks. US Geological Survey Bulletin, 1144-E, p. 55.

Matter, A. (1964). Sedimentologische Untersuchungen im östlichen Napfgebiet (Entlebuch-Tal der Grossen Fontanne, Kt. Luzern). *Eclogae Geologicae Helveticae, 57*(2), 315–329.

Miall, A. D. (1978). Lithofacies types and vertical profile models in braided rivers: A summary. In A.D. Miall (Ed.), *Fluvial sedimentology* (pp. 605–625). Canadian Society of Petroleum Geologists, Memoir 5.

Miall, A. D. (1996). *The geology of fluvial deposits. Sedimentary facies, basin analysis, and petroleum geology* (p. 582). Berlin: Springer.

Molinaroli, E., & Basu, A. (1993). Toward quantitative provenance analysis: A brief review and case study. In M. J. Johnsson & A. Basu (Eds.), *Processes controlling the composition of clastic sediments* (pp. 223–233). Geological Society of America Special Paper 284.

Nemec, W., & Steel, R. J. (1984). Alluvial and costal conglomerates: Their significant features and some comments on gravelly mass-flow deposits. In E.H. Koster and R.J. Steel (Eds.), *Sedimentology of gravel and conglomerates* (pp. 1–31). Canadian Society of Petroleum Geologists, Memoir, 10.

Norton, K. P., von Blanckenburg, F., Schlunegger, F,. Schwab, M., & Kubik, P. W. (2008). Cosmogenic nuclide-based investigation of spatial erosion and hillslope channel coupling in the transient foreland of the Swiss Alps. *Geomorphology 95*(3-4), 474–486.

Pavoni, N. (1957). Geologie der Zürcher Molasse zwischen Albiskamm und Pfannenstiel. *Vierteljahrsschrift der Naturforschenden Gesellschaft in Zürich, 102*(5), 117–315.

Penck, A., & Brückner, E. (1909). *Die Alpen im Eiszeitalter* (p. 716). Leipzig: Tauchnitz.

Petit, C., Campy, M., Chaline, J., & Bonvalot, J. (1996). Major palaeohydrographic changes in Alpine foreland during the Pliocene–Pleistocene. *Boreas, 25,* 131–143.

Poser, H., & Hövermann, J. (1952). Beiträge zur morphometrischen und morphologischen Schotteranalyse. *Abhandlungen der Braunschweigischen Wissenschaftlichen Gesellschaft, 4,* 12–36.

Portenga, E. W., & Bierman, P. R. (2011). Understanding Earth's eroding surface with 10Be. *GSA Today, 21*(8), 4–10.

Preusser, F., Graf, H. R., Keller, O., Krayss, E., & Schlüchter, C. (2007). Quaternary glaciation history of northern Switzerland. *E&G Quaternary Science Journal, 60*(2–3), 282–305.

Preusser, F., Graf, H. R., Keller, O., Krayss, E., & Schlüchter, C. (2011). Quaternary glaciation history of northern Switzerland. *E&G Quaternary Science Journal, 60*(2–3), 282–305.

Preusser, F., Reitner, J., & Schlüchter, C. (2010). Distribution, geometry, age and origin of overdeepened valleys and basins in the Alps and their foreland. *Swiss Journal of Geosciences, 103,* 407–426.

Rentzel, P., Preusser, F., Pümpin, C., & Wolf, J.-J. (2009). Loess and palaeosols on the High Terrace at Sierentz (France), and implications for the chronology of terrace formation in the Upper Rhine Graben. *Swiss Journal of Geosciences, 102,* 387–401.

Repka, J. L., Anderson, R. S., & Finkel, R. C. (1997). Cosmogenic dating of fluvial terraces, Fremont River, Utah. *Earth and Planetary Science Letters, 152,* 59–73.

Richter, M. (1930). Der ostalpine Deckenbogen. *Jahrbuch der Geologischen Bundesanstalt, 80,* 497–540.

Sartori, M., Gouffon, Y., & Marthaler, M. (2006). Harmonisation et définition des unités lithostratigraphiques briançonnaises dans les nappes penniques du Valais. *Eclogae Geologicae Helvetiae, 99,* 363–407.

Schielein, P., Schellmann, G., Lomax, J., Preusser, F., & Fiebig, M. (2015). Chronostratigraphy of the Hochterrassen in the lower Lech valley (Northern Alpine Foreland). *E&G Quaternary Science Journal, 64*(1), 15–28.

Schlüchter, C. (1976). *Geologische Untersuchungen im Quartär des Aaretals südlich von Bern (Stratigraphie, Sedimentologie, Paläontologie)* (p. 148). N.F.: Beiträge zur Geologischen Karte der Schweiz.

Schlüchter, C. (1988/89). A non-classical summary of the quaternary stratigraphy in the northern alpine foreland of Switzerland. *Bulletin de la Société Neuchâteloise de Géographie*, *32–33*, 143–157.

Schlüchter, C. (1989). Eiszeitliche Lockergesteine—Geologie, Genese und Eigenschaften. Ein Beitrag zu den Beziehungen zwischen fundamentaler und angewandter Eiszeitgeologie. *Habilitationsschrift,* Eidgenössische Technische Hochschule Zürich, Zurich, p. 162.

Schlüchter, C. (2004). The Swiss glacial record—a schematic summary. In J. Ehlers & P. L. Gibbard (Eds.), *Quaternary glaciations—extent and chronology, part I: Europe* (pp. 413–418). Amsterdam: Elsevier.

Schlunegger, F., Slingerland, R., & Matter, A. (1998). Crustal thickening and crustal extension as controls on the evolution of the drainage network of the central Swiss Alps between 30 Ma and the present: Constraints from the stratigraphy of the North Alpine Foreland Basin and the structural evolution of the Alps. *Basin Research, 10,* 197–212.

Schumacher, M. E. (2002). Upper Rhine Graben: Role of preexisting structures during rift evolution. *Tectonics, 21*, 6-1–6-17.

Siame, L., Bellier, O., Braucher, R., Sébrier, M., Cushing, M., Bourlès, D., et al. (2004). Local erosion rates versus active tectonics: Cosmic ray exposure modelling in Provence (southeast France). *Earth and Planetary Science Letters, 220,* 345–364.

Siegenthaler, C., & Huggenberger, P. (1993). Pleistocene Rhine gravel: Deposits of a braided river system with dominant pool preservation. In J. Best and C. Bristow (Eds.), *Braided rivers* (pp. 147–162). Geological Society Special Publication, 75.

Sinn, P. (1972). Zur Stratigraphie und Paläogeographie des Präwürm im mittleren und südlichen Illergletscher-Vorland. *Heidelberger geographische Arbeiten, 37,* 159.

Sneed, E. D., & Folk, R. L. (1958). Pebbles in the Colorado River, Texas, a study in clast morphogenesis. *Journal of Geology, 66,* 114–150.

Spell, T. L., & McDougall, I. (1992). Revisions to the age of the Brunhes–Matuyama boundary and the Pleistocene geomagnetic polarity timescale. *Geophysical Research Letters, 19*(12), 1181–1184.

Spicher, A. (1980). Tektonische Karte der Schweiz. Schweizerische Geologische Kommission.

Stone, J. O. (2000). Air pressure and cosmogenic isotope production. *Journal of Geophysical Research, 105*(B10), 23753–23759.

Stone, J.O., Allan, G.L., Fifield, L.K., & Cresswell, R.G. (1996). Cosmogenic chlorine-36 from calcium spallation. *Geochimica et Cosmochimica Acta, 60*(4), 679–692.

Ustaszewski, K., & Schmid, S. M. (2007). Latest Pliocene to recent thick-skinned tectonics at the Upper Rhine Graben—Jura Mountains junction. *Swiss Journal of Geosciences, 100,* 293–312.

Verderber, R. (1992). Quartärgeologische Untersuchungen im Hochrheingebiet zwischen Schaffhausen und Basel. Ph.D. dissertation, Albert-Ludwigs-Universität Freiburg, Freiburg i.B., Germany, p. 169.

Weltje, G. V., & von Eynatten, H. (2004). Quantitative provenance analysis of sediments: Review and outlook. *Sedimentary Geology, 171,* 1–11.

Wittmann, O., Hauber, L., Fischer, H., Rieser, A., & Staehlin, P. (1970). Geologischer Atlas der Schweiz, 1:25,000, Blatt 1047 Basel.

Wittmann, H., von Blanckenburg, F., Kruesmann, T., Norton, K. P., & Kubik, P. W. (2007). Relation between rock uplift and denudation from cosmogenic nuclides in river sediment in the Central Alps of Switzerland. *Journal of Geophysical Research, 112*, F04010. doi:10.1029/2006JF000729.

Zollinger, G. (1991). Zur Landschaftsgenese und Quartärstratigraphie am südlichen Oberrhein—am Beispiel der Lössdeckschichten der Ziegelei in Allschwil (Kanton Basel-Landschaft). *Eclogae Geologicae Helveticae, 84,* 739–752.

Zreda, M. G., & Phillips, F. M. (1994). Surface exposure dating by cosmogenic Chlorine-36 accumulation. In C. Beck (Ed.), *Dating in exposed and surface contexts* (pp. 161–183). Albuquerque: University of New Mexico Press.